Proceedings of the XII International Symposium on Dynamic Problems of Mechanics (DINAME 2007),
Varoto, P. S. and Trindade, M. A. (Editors), ABCM, Ilhabela, SP, Brazil, February 26 - March 2, 2007

Considerations on Dynamic Model of a Parallel Architecture and its influence in Optimum Path Planning

Oliveira P.J. [1], Saramago S.F.P. [2], Carvalho J.C.M. [2], Carbone G. [3], Ceccarelli M. [3]

[1] Federal University of Goiás, Av. Lamartine Pinto Avelar,1120 – 75709-220, Catalão (G), Brazil

[2] Federal University of Uberlândia, Av. João Naves de Àvila, 2160 – 38408-100, Uberlândia (MG), Brazil

[3] Laboratory of Robotics and Mechatronics, University of Cassino, Via Di Basio, 43 – 03043, Cassino (FR), Italy

Abstract: The main objective of this work is obtains an optimal trajectory of a parallel architecture by using a multi-objective optimization problem, which is proposed taking into account the mechanical energy of the actuators, the total traveling time and jerk. These objectives are in conflict with each other, mainly in the applications where the manipulator should work with high velocities. The trajectory is calculated assuming that the input angles are given by a function of the time, that is represented by an uniform B-splines. The kinematic modelling is obtained by deriving the trajectory equation according the time. The analytic model for the inverse dynamics of CaPaMan uses the Newton-Euler equations. The dynamic model will be able to calculate the energy accurately. In many cases are enough to consider the forces acting on the mobile platform (simplified dynamic model), but as more robust manipulators are considered becomes also important to consider the forces on each articulated parallelogram of legs (complete dynamic model). This procedure has been applied to a practical example for a path planning of a parallel manipulator named as CaPaMan (Cassino Parallel Manipulator). Two cases are studied: the first considers the data of a built prototype at LARM (Laboratory of Robotics and Mechatronics at Cassino) and the second test referes to a robust hypothetical manipulator. The obtained results are compared when the two dynamic models are applied .

Keywords: Robotics, Parallel Manipulators, Path Planning , Dynamic Model.

NOMENCLATURE

a_i = length of the frame link, m
$\boldsymbol{a_p}$ = acceleration of the central point P
b_i = length of the input crank, m
$B_{k,d}$ = polynomials functions of the cubic B-splines
c_i = length of the coupler link, m
d_i = length of the follower crank,m
E = total energy of the manipulator, Nm/s^2
E_0 = initial energy spent to travel the initial trajectory, Nm/s^2
h_i = length of the connecting bar, m
$\boldsymbol{F_i}$ = reaction force acting at points H_i of the mobile platform, N
$\boldsymbol{F_{ext}}$ = external force, N
$\boldsymbol{G}$ = mobile platform weight, N
f= multi-objective function
F = the sum of the reaction force, N
FP =fixed base
K_1, K_2 , K_3 = weighting coefficients of the multi-objective function
H_i = position of spherical joints
I = inertia matrix of the mobile platform
J = jerk (acceleration variation), rad/s^3
J_o = jerk for the initial trajectory, rad/s^3
m_{hi}, m_{bi} , m_{ci} = masses of the links h_i, b_i and c_i, Kg
M = mobile platform mass, Kg
$\boldsymbol{N}$ =the resultant torque due to the forces $\boldsymbol{F_i}$,Nm
$\boldsymbol{N_{ext}}$ = external torque, Nm
MP = mobile platform
P = center point of the mobile platform
P_0 , P_m = initial and final point of the trajectory
p^i_k = B-splines control points
r_b = size of the base, m
r_p = size of the mobile platform, m
R = rotation matrix
s_i = coordinate displacement of the passive prismatic joint, m
T_0 = total traveling time for the initial trajectory, s
Tt = total traveling time, s
Tt^l , Tt^u = lower and upper limits for the total traveling time, s
t = time variable, s
x, y, z = coordinates of center P point

Greek Symbols

α_i = input crank angles, deg
$\alpha_i(t)$ = manipulator's trajectory, deg
α_i^l , α_i^u = lower and upper limits for each crank angle, deg
$\dot{\alpha}_i(t)$ = time derivative of the input crank angles, rad/s
δ_i = the structural rotation angle between OX_1 and OX_i, rad
θ, φ and ψ = Euler angles, rad
τ_i = actuator torque on the input crank shaft, Nm
τ_i^l ,τ_i^u = lower and upper limits for the actuator torque on input crank shaft, Nm
τ_{Mi} = input torque due to the articulated parallelogram, Nm
τ_{Pi} = input torque due to dynamic effect of the mobile platform, Nm
$\dot{\boldsymbol{\omega}}$ = mobile platform angular accelerations, rad/s^2
$\boldsymbol{\omega}$ = mobile platform angular velocity, rad/s

INTRODUCTION

Parallel manipulator is a closed-loop mechanism in which the end-effector (mobile platform) is connected to the base by at least two independent kinematic chains. Parallel manipulators are of great interest mainly because they present advantages in several applications, showing low inertia, high stiffness, great resistance, high positioning accuracy, load capacity larger than serial manipulators and they can be operated to high-speeds and accelerations. Parallel architectures can be applied in many areas, such as airplane simulators, mining machines and walking machines like those presented in Stewart (1965), Clavel (1987, 1988), Pierrot et al. (1991), Merlet and Gosselin (1991), Jacquet et al. (1992), Romiti and Sorli (1992), Lallemand et al. (1997), Byun and Cho (1997), Ceccarelli (1997), Portman and Sandler (1999), (Tsai, 1999), Kim and Tsai (2002), Gosselin et al. (2004) and Di Gregório and Parenti-Castelli (2004). At LARM, Laboratory of Robotics and Mechatronics in Casino, Italy, a parallel mechanism was built with three degrees of freedom, called CaPaMan (Cassino Parallel Manipulator). A prototype has been built and the performance and suitable formulation for kinematics, statics and dynamics have been investigated and results are reported in Carvalho and Ceccarelli (2001).

When repetitive processes are imposed, it is important to develop a methodology to move a robot along a specified optimum path. This path can be seen as a necessary sequence of movements that the robot needs to perform a task. The motion must be smooth as it is possible, without suddenly changes on positions, velocities and accelerations. If sudden motion takes place, the system requires high energy to execute it. For example when collisions occurs between the robot end-effector and an object. Studies have been made in order to obtain optimum trajectories for serial and parallel robot architectures considering a constrained workspace, a minimum time, a minimum displacement and so on Brobow et al. (1985), Shiller and Lu (1992), Constantinescu and Croft (2000) and Saramago and Ceccarelli (2002). In this work, a general formulation has been proposed for optimum path planning for parallel manipulators by using a multi-objective optimization problem, which is written taking into account the mechanical energy of the actuators, the total traveling time and jerk. These objectives are in conflict with each other, mainly in the applications where the manipulator should work to high velocities. The trajectory is calculated assuming that the input angles are given by a function of the time, that are represented by an uniform B-splines. The kinematic modelling is obtained by deriving the trajectory equation according the time. The analytical model for the inverse dynamics of CaPaMan uses the equations of Newton-Euler.

The main objective of this work is to show the importance of the dynamical model to obtain an optimized trajectory, since it enable to calculate the energy accurately. In many cases are enough to consider the forces acting on the mobile platform (simplified dynamic model), but as more robust manipulators are considered becomes also important to consider the forces on each leg (complete dynamic model). Two cases are studied: the first one considers the data of the prototype built at LARM (Laboratory of Robotics and Mechatronics in Cassino) and the second one tests a robust hypothetical manipulator. The obtained results are compared when the two dynamic models are applied

THE CAPAMAN ARCHITECTURE

The Cassino Parallel Manipulator – CaPaMan is a three d.o.f. parallel that is manipulator composed by a fixed base FP and a mobile platform MP which are connected by three mechanism legs. Each mechanism leg is composed of an articulated parallelogram AP where on the coupler link is installed a passive prismatic joint SJ, a vertical rod CB that connects to the mobile platform through a spherical joint BJ. Each mechanism leg is rotated $2\pi/3$ with respect to the neighboring one as shown in the Figure 1a.

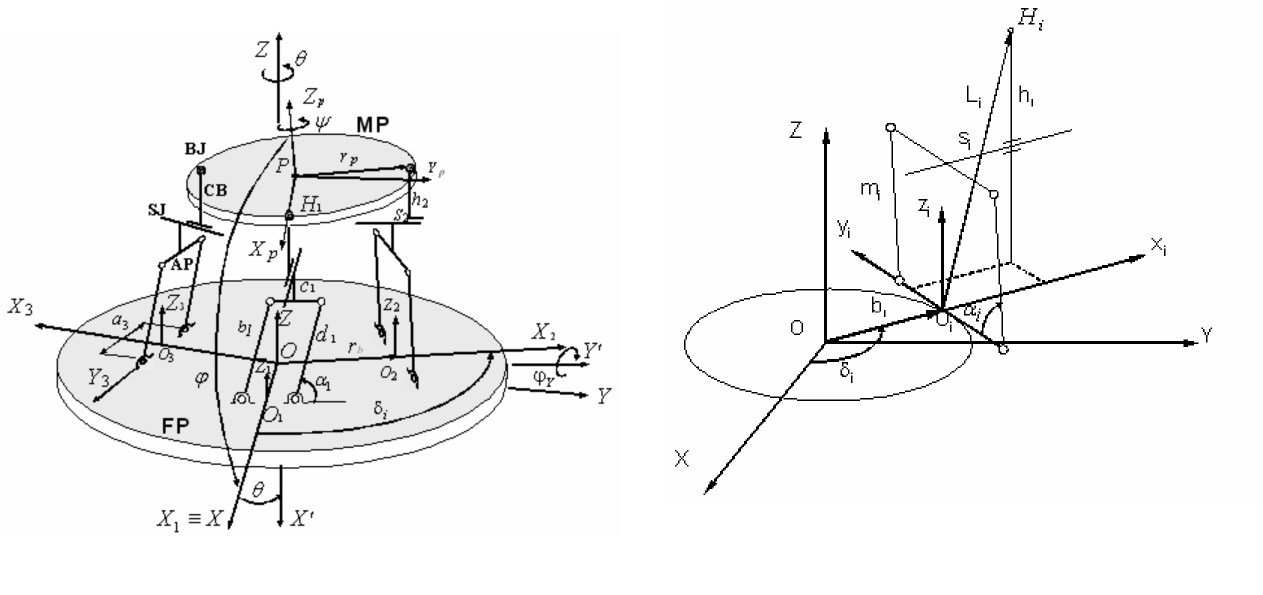

a) b)

Figure 1. a) Kinematic chain of CaPaMan. b) Parameters associated to the *i-th* leg.

In order to describe the CaPaMan's kinematic behavior, five reference frames are defined: an inertial frame *OXYZ* has been assumed to be fixed to the FP, a moving frame $PX_pY_pZ_p$ has been attached to the MP and one reference frame

$O_iX_iY_iZ_i$ (i=1,2,3) has been assumed fixed at the center of the fixed link of each articulated parallelogram. The inertial frame *OXYZ* has been assumed with X-axis as coincident with the line joining *O* to O_1; Z-axis is orthogonal to FP plane and Y-axis is directed to give a Cartesian frame. The moving frame $PX_pY_pZ_p$ has been assumed with X_p-axis as coincident to the line joining *P* to H_1, Z_p-axis orthogonal to MP and Y_p-axis to give a Cartesian frame. On each parallelogram reference frame the X_i-axis is orthogonal to the mechanism plane; the Y_i-axis is coincident with link frame direction and the Z_i-axis lies on the mechanism plane. Thus, each X_i-axis is rotated of 2π/3 from the others.

The linkage parameters of a *i-th* (i=1,2,3) leg mechanism are identified by the length of the frame link a_i, b_i is the length of the input crank; c_i is the length of the coupler link; d_i is the length of the follower crank and h_i is the length of the connecting bar. The size of the mobile platform is given by the distance r_p from the center point P to joint points H_i. Similarly r_b represents the size of the base being the distance between its center *O* and the middle point O_i of the frame link a_i. In addition, s_i is the coordinate displacement of the passive prismatic joint; the angle δ_i is the structural rotation angle between OX_1 and OX_i as well as between PH_1 and PH_i that are equal to $\delta_1=0$, $\delta_2=2\pi/3$ and $\delta_3=4\pi/3$, and the kinematic variables are the input crank angles α_i (i=1,2,3) of the articulated parallelograms.

The orientation of the mobile platform MP can be described with respect to the inertial frame *OXYZ* through the Euler angles θ, φ and ψ in which θ is the first rotation, about the Z-axis; the tilting rotation φ_y about the Y'-axis, which is the Y-axis after a θ rotation. The third rotation ψ is about the Z"-axis, which is coincident with the Z_p-axis. φ is the complementary angle of φ_y as shown in Figure 1a. It is possible to derive the Euler angles expressions as function of the y_i and z_i coordinates of H_i points as shown by Ceccarelli (1997), Fig. 1b.

The rotation matrix *R* from the moving frame $PX_pY_pZ_p$ to the fixed frame *OXYZ* can be obtained from Euler's angles θ, φ and ψ remembering that $\varphi_y = \pi/2 - \varphi$:

$$R = \begin{pmatrix} \cos\theta\ \sin\varphi\ \cos\psi - \sin\theta\ \sin\psi & -\cos\theta\ \sin\varphi\ \sin\psi - \sin\theta\ \cos\psi & \cos\theta\ \cos\varphi \\ \sin\theta\ \sin\varphi\ \cos\psi + \cos\theta\ \sin\psi & -\sin\theta\ \sin\varphi\ \sin\psi + \cos\theta\ \cos\psi & \sin\theta\ \cos\varphi \\ -\cos\varphi\ \cos\psi & \cos\varphi\ \sin\psi & \sin\varphi \end{pmatrix} \tag{1}$$

The direct displacement analysis can be derived from Figure 1a through a closed-form formulation of the spherical joints coordinates, represented by points H_1, H_2, and H_3, because the center *P* point of the mobile platform is defined by the center of the equilateral triangle which vertices are its articulation points H_1, H_2, and H_3. Thus, the coordinates of center *P* point can be given as

$$\begin{aligned} x &= (y_3 - y_2)/\sqrt{3} - \left[r_p(1-\sin\varphi)\ \cos(\psi-\theta)\right]/2 \\ y &= y_1 - r_p(\sin\psi\cos\theta + \cos\psi\ \sin\varphi\ \ \sin\theta) \\ z &= (z_1 + z_2 + z_3)/3 \end{aligned} \tag{2}$$

The components of the velocity and acceleration of *P* point can be obtained by the first and second derivatives of the *x*, *y*, and *z* expressions. The components ω_x, ω_y and ω_z of the mobile platform angular velocity ω can be written in terms of Euler's angles and their time derivatives as

$$\begin{pmatrix} \omega_x \\ \omega_y \\ \omega_z \end{pmatrix} = \begin{pmatrix} -\cos\varphi\ \cos\psi & \sin\psi & 0 \\ \cos\varphi\ \sin\psi & \cos\psi & 0 \\ \sin\varphi & 0 & 1 \end{pmatrix} \begin{pmatrix} \dot\theta \\ \dot\varphi \\ \dot\psi \end{pmatrix} \tag{3}$$

THE SIMPLIFIED DYNAMIC MODEL

The simplified dynamic model of CaPaMan has been computed by considering only the dynamic effects of the mobile platform. The Newton-Euler equations can be formulated considering the MP as rigid body, and its orientation, position, velocities and accelerations related to the inertial reference frame *OXYZ*. Thus, the Newton-Euler equations representing the dynamic equilibrium for the MP, by assuming that $r_b = r_p$, can be written as

$$\boldsymbol{F} + \boldsymbol{F_{ext}} + \boldsymbol{G} = \boldsymbol{F_{in}} \qquad \text{and} \qquad N + N_{ext} = N_{in} \tag{4}$$

Where $\boldsymbol{F_{ext}}$ is the external force, $\boldsymbol{N_{ext}}$ is the external torque, $\boldsymbol{G}$ is the mobile platform weight; $\boldsymbol{F}$ is the sum of the reaction force $\boldsymbol{F_i}$ (i=1, 2,3) acting at points H_i of the MP and $\boldsymbol{N}$ is the resultant torque due to the forces $\boldsymbol{F_i}$, respected to the fixed reference frame OXYZ.

Moreover, it must be considered that:

$$\mathbf{F_{in}} = M\,\mathbf{a}_P\,,\ \ \mathbf{N_{in}} = I\dot{\boldsymbol{\omega}} + \boldsymbol{\omega}\times I\,\boldsymbol{\omega}\,,\ \ \boldsymbol{F} = \sum_{i=1}^{3}\boldsymbol{F_i}\ \text{, and}\ \ \boldsymbol{N} = \sum_{i=1}^{3}\left(r_p R\,\boldsymbol{u}_{\mathbf{ip}}\right)\times\boldsymbol{F_i}\ \ \text{for}\ \ (i=1,2,3) \tag{5}$$

Where M is the mass of MP; $\boldsymbol{a_p}$ is the acceleration of the central point P, $\dot{\boldsymbol{\omega}}$ and $\boldsymbol{\omega}$ are the angular accelerations and angular velocities, respectively, and I is the inertia matrix of the mobile platform. The inertia matrix I can be determined as $I = R\,I_c\,R^t$ by using the rotation matrix R, its transpose matrix R^t, and the inertia matrix I_c of MP with respect to its reference frame $PX_pY_pZ_p$.

When the friction in the joints is neglected, the only forces applied to the articulated points H_i by rods CB are those which are contained in the plane of the articulated parallelogram. These joint forces have only components F_{iy} and F_{iz} (i=1,2,3). Equations (4) can be solved in a closed form formulation to obtain the force components F_{iy} and F_{iz} as depicted in Ceccarelli and Carvalho (1999, 2001).

From Figures 1a and 2a, the torque τ_{Pi} (i=1,2,3) on the input crank shaft of each articulated parallelogram can be obtained from the dynamic equilibrium of the leg mechanism as

$$\tau_{Pi} = \frac{F_{iz}\,b_i\,sin(2\,\alpha_i\,)}{2\,sin\,\alpha_i} - F_{iy}\,b_i\left(\frac{h_i}{c_i\,tan\,\alpha_i}+1\right)\left(1-\frac{h_i}{h_i\,cos\,\alpha_i + c_i\,sin\,\alpha_i}\right)sin\,\alpha_i \qquad (i=1,2,3) \tag{6}$$

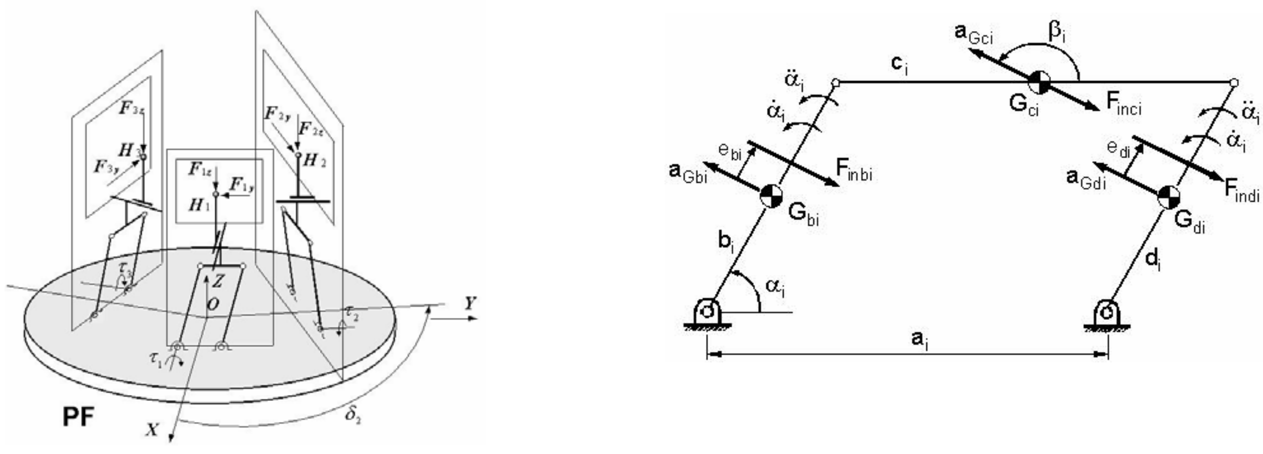

a) b)

Figure 2. a) Forces acting at the spherical joints. b) Forces in the *i-th* articulated parallelogram (i=1,2,3).

THE COMPLETE DYNAMIC MODEL

The complete dynamic model of CaPaMan is obtained by considering both the mobile platform dynamic effects and articulated parallelogram dynamic effects. For the dynamic analysis of the articulated parallelograms one can assume that the linear accelerations of the mass centers and angular accelerations of each segment were obtained from the kinematic analysis of the articulated parallelograms and the mass centers of links are coincident with the figures centers. By using the kinetostatic analysis of mechanisms, the dynamic equilibrium in the presence of the three inertia forces $\boldsymbol{F_{inbi}} = -m_{bi}\,\boldsymbol{a_{Gbi}}$, $\boldsymbol{F_{inci}} = -m_{ci}\,\boldsymbol{a_{Gci}}$ and $\boldsymbol{F_{indi}} = -m_{di}\,\boldsymbol{a_{Gdi}}$, whose application points are obtained by offsets e_{bi}, e_{ci}, and e_{di}, from the mass center of links b_i, c_i and d_i, respectively, as shown in Fig. 2b, are given by:

$$e_{bi} = \frac{I_{Gbi}\,\dot{\omega}_{bi}}{F_{inbi}} = \frac{I_{Gbi}\,\ddot{\alpha}_i}{F_{inbi}}\,; \quad e_{ci} = \frac{I_{Gci}\,\dot{\omega}_{ci}}{F_{inci}} = 0\,; \quad e_{di} = \frac{I_{Gdi}\,\dot{\omega}_{di}}{F_{indi}} = \frac{I_{Gdi}\,\ddot{\alpha}_i}{F_{indi}} \tag{7}$$

Using the superposition principle, the effects of the inertia forces of links can be calculated separately and then to determine the combined effect. The analysis can be taken by using the free body diagram.

The input torque τ_{Mi} due to the articulated parallelogram is obtained from the total effect of the inertia of the three movement links and the gravitational effect of the links b_i, d_i , h_i , and c_i. Thus, the input torque τ_{Mi} can be written as:

$$\tau_{Mi} = 2l_{bi} F_{inbi} \sin(\alpha_i - \beta_i + \pi) + F_{23i}\, b \sin(\alpha_i + \pi - \gamma_i) + b\left[m_{bi} \cos\alpha_i + \frac{(m_{ci} + m_{hi}) \sin 2\alpha_i}{2 \sin\alpha_i} \right] g \tag{8}$$

with

$$l_{bi} = \frac{b}{2} + \frac{I_{Gbi}\, \ddot{\alpha}_i}{F_{inbi}} \frac{1}{\sin(\alpha_i - \beta_i + \pi)}, \qquad \gamma_i = tg^{-1}\left\{ \frac{\left[\dfrac{F_{inci} \sin(\beta_i + \pi)}{2}\right]}{F_{inci}\left[\cos(\beta_i + \pi) + \dfrac{\sin(\pi - \beta_i)}{2 \tan\alpha_i}\right]} \right\}$$

$$F_{23i} = \left| \sqrt{\left\{ F_{inci}\left[\cos(\beta_i + \pi) + \frac{\sin(\pi - \beta_i)}{2 \tan\alpha_i}\right]\right\}^2 + \left[\frac{F_{inci} \sin(\beta_i + \pi)}{2}\right]^2} \right| \tag{9}$$

Where the angles β_i define the direction of the acceleration of the mass center of the *i-th* link with respect to the horizontal axis, assumed to be positive counter-clockwise. Similarly, γ_i defines the direction of the reaction force vector acting on the ground pivot of link in the base of the segment d_i.

Since the obtained dynamic equations are algebraic and linear in the inertia forces, the principle of superposition can be applied. Thus, the dynamic effect of the mobile platform can be superposed to the dynamic effect of the articulated parallelogram. The total torque τ_i on the input crank shaft of each articulate parallelogram can be obtained by adding the torques τ_{Pi} and τ_{Mi} that are obtained from the dynamic analysis of the mobile platform and of the articulated parallelograms, given by Eqs. (6) and (8), respectively. Thus

$$\tau_i = \tau_{Pi} + \tau_{Mi} \qquad (i=1,2,3) \tag{10}$$

TRAJECTORY FORMULATION

The kinematic variables which are defined by the input crank angles α_i (i=1,2,3) of the articulated parallelogram can be described by uniform cubic B-spline, using concordance functions, in the form

$$\alpha_i(t) = \sum_{k=0}^{n_p} p_k^i B_{k,d}^i(t), \quad t_o \le t \le t_f, \quad n_p \ge 3, \quad (i=1,2,3) \tag{11}$$

Where p^i_k are n_p+1 control points related to each trajectory α_i and $B_{k,d}$ are polynomials defined by Cox-Boor recurrence formulas (Foley et all ,1990). For the cubic spline (d=4), $B_{k,d}$ are:

$$B_{k,1}(t) = \begin{cases} 1 & if \ t_k \le t \le t_{k+1} \\ 0 & out \end{cases}, \quad B_{k,d}(t) = \frac{t - t_k}{t_{k+d-1} - t_k} B_{k,d-1}(t) + \frac{t_{k+d} - t}{t_{k+d} - t_{k+1}} B_{k+1,d-1}(t) \tag{12}$$

Each concordance function is defined on d subintervals of the total interval. The set of the extreme points of the subintervals t_i, is called knot points vector. As $\alpha_i(t)$ is constituted by polynomials, its derivatives of order j related to t can be obtained as:

$$\frac{d^j \alpha_i(t)}{dt^j} = \sum_{k=0}^{n_p} p_k^i \frac{d^j B_{k,d}^i}{dt^j} \tag{13}$$

Thus, the first and second derivatives related to the time are given by:

$$\dot{\alpha}_i(t) = \sum_{k=0}^{n_p} p_k^i \dot{B}_{k,d}^i(t), \qquad \ddot{\alpha}_i(t) = \sum_{k=0}^{n_p} p_k^i \ddot{B}_{k,d}^i(t) \quad (i=1,2,3) \tag{14}$$

FORMULATION FOR THE OPTIMAL PATH PLANNING

In multicriteria optimization one deals with a design variable vector x, which satisfies all the constraints and makes as small as possible the scalar performance index that is calculated by taking into account the m components of an objective function vector *f(x)*. An important feature of such multiple criteria optimization problem is that the optimizer has to deal with conflicting objectives. Solutions to multicriteria optimization problems can be found in different ways by defining the so-called substitute problems. Substitute problems represent different forms of obtaining the corresponding scalar objective function (Eschenauer et al, 1990). Weighting Objectives is one of the most usual (and simple) substitute models for multiobjective optimization problems. It permits a preference formulation that is independent from the individual minimum for positive weights. The performance index or utility function is here determined by the linear combination of the criteria *f1,...,fm* , together with the corresponding weighting factors *K1* ,..., *Km* . It is usually assumed that $0 \le Kj \le 1$ and $\Sigma\, Kj = 1$.

To optimize a manipulator operation, the energy aspect can be considered as one of the most significant, since the energy formulation considers both the dynamics and kinematics characteristics of the manipulator. In other way, to maximize the operation speed means to minimize the traveling time. But, a minimal time represents an increment on jerk values. Thus, these three characteristics, the optimal traveling time, the minimum jerk and minimum mechanical energy of the actuators, can be considered to build a multi-objective function in an optimization problem that can be defined as

$$\text{Minimize } f = K_1 \frac{E}{E_0} + K_2 \frac{Tt}{T_0} + K_3 \frac{J}{J_0} \tag{15}$$

$$\text{Subject to } \alpha_i^l \le [\alpha_i(t)] \le \alpha_i^u \;,\; Tt^l \le Tt \le Tt^u \;,\; (i=1,2,3) \tag{16}$$

In which the control points p^i_k of each trajectory are the design variables and the total energy of the manipulator can be written as

$$E = \int_0^{Tt} \sum_{i=1}^{3} [\tau_i(t)\, \dot{\alpha}_i(t)]\, dt, \quad \text{with} \quad \tau_i^l \le \tau_i \le \tau_i^u \tag{17}$$

and

$$J = max \left| \frac{\partial^3 \alpha_i(t)}{\partial t} \right| \qquad (i=1,2,3) \tag{18}$$

Where τ_i is the actuator torque on the *i-th* input crank shaft, given by Eq. (10); α_i (t) is the *i-th* joint variable, Eq. (11), and $\dot{\alpha}_i(t)$ its time derivative given by Eq. (13); *t* is the time variable in the interval [0, *Tt*] for the path between P_o and P_m; *Tt* is the total traveling time at the end point P_m when *t*=0 is assumed at the initial point P_0 . The side constraints have been formulated in Eq. (16) given by lower and upper limits for each crank angle ($\alpha_i^{\ l}$ and α_i^u), the lower and upper limits for the total traveling time (Tt^l and Tt^u), and the lower and upper limits for the actuator torque on the *i-th* input crank shaft ($\tau_i^{\ l}$ and $\tau_i^{\ u}$). In Equation (15) K_1, K_2 and K_3 are weighting coefficients of the multi-objective function, E_0, T_0 and J_0 are reference values. The jerk (acceleration variation) is obtained using Eq. (18). The proposed formulation, Eqs. (15) to (18) requires the computation and consideration of the manipulator kinematics and dynamics.

In the optimization process, a general analysis code was developed in Matlab®, and it was coupled to the optimization program. This analysis code allows to obtain the manipulator's trajectory modeled by splines according to the Eq. (11), the kinematics model according to Eqs. (1), (2), and (3), the dynamic model given by Eqs. (4) to (10) and the energy using Eq. (17). In the optimization process it was applied Genetic Algorithms through the program GAOT (Genetic Algorithms Optimization on Toolbox) developed for Houck et al (1995).

NUMERICAL SIMULATION

To verify the importance of the dynamical model, two cases are studied: the first considers the data of the CaPaMan prototype and the second test a robust hypothetical manipulator. The obtained results are compared when the two dynamic models are applied (simplified and complete models). It is considered that the robot is initially in rest and it is completely stopped at the end of the trajectory, that is to say, $\dot{\alpha}_i(0) = \dot{\alpha}_i(T_t) = 0$, i=1,2,3. The weighting coefficients of the multi-objective function *f*, in Eq. (15), are adopted as: k_1=0.3, k_2=0.3 and k_3=0.4. The total traveling time for the initial trajectory is T_0 =0.3 s. The constraints given by Eqs. (16) are assumed as: $60^o \le \alpha_1(t) \le 90^o$; $50^o \le \alpha_2(t) \le 120^o$; $80^o \le \alpha_3(t) \le 100^o$; $0{,}1\, s \le Tt \le 0.5\, s$.

Application 1: CaPaMam prototype

The dimensional data of CaPaMan prototype are related in Table 1. The mobile platform has mass M=2. 912 Kg, the segments h_i, b_i and c_i have masses respectively the same to m_{hi}=0.100 Kg, m_{bi}=0. 103 Kg and m_{ci}=0. 547 Kg.

Table 1 – Dimensional parameters of the CaPaMan prototype

$a_i = c_i$ [mm]	$b_i = d_i$ [mm]	h_i [mm]	$r_P = r_b$ [mm]	s_i [mm]
200	80	116	109.5	-50; 50

The initial and optimal values for the simplified dynamical model are reported in Table 2 and for the complete dynamical model in Table 3. Observe that the energy value was increased when the complete model was used because the articulated parallelogram dynamic effects were considered. For the both cases the results showing that there is a significant improvement of the performances index by using genetic algorithms.

Table 2 – Optimal results for the CaPaMan prototype (simplified dynamical model)

	Multi –objective function	Energy [Nm/s^2]	Total traveling time [s]	Jerk [rad/s^3]
Initial value	1.00	210.99	0.30	826.0
Optimal value	0.70	87.66	0.48	202.0
Performance Index	30.0 %	58.5 %	-	75.5 %

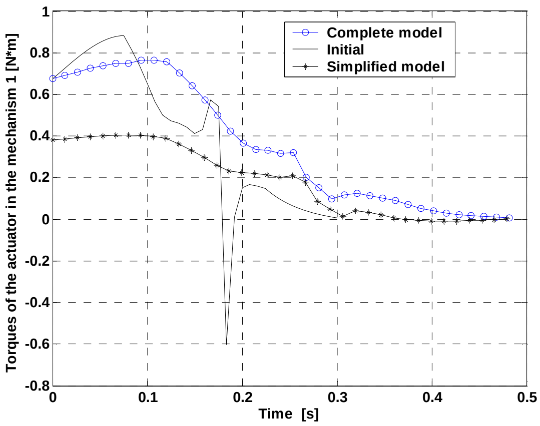

(a)

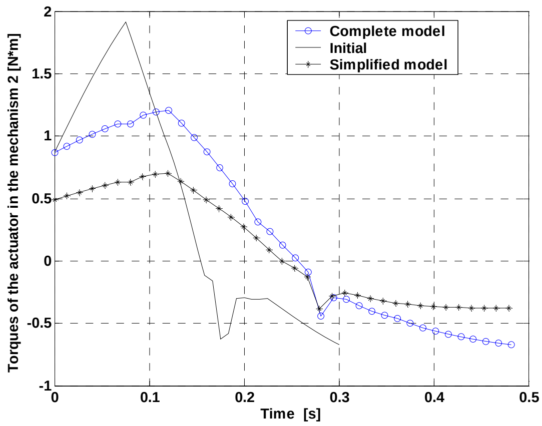

(b)

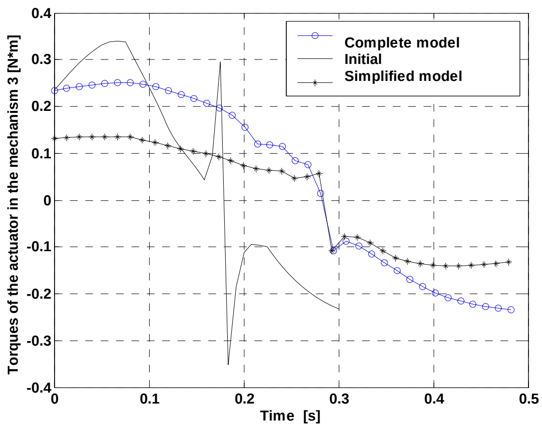

(c)

Figure 3- Initial and optimum curves of the actuator torque for CaPaMan prototype obtained by simplified and complete dynamic models: (a) leg mechanism 1; (b) leg mechanism 2; (c) leg mechanism 3.

Table 3 – Optimal results for the CaPaMan prototype (complete dynamical model)

	Multi –objective function	Energy [Nm/s^2]	Total traveling time [s]	Jerk [rad/s^3]
Initial value	1.00	316.99	0.30	827.0
Optimal value	0.71	144.69	0.48	199.0
Performance Index	29.0 %	54.4 %	-	76.0 %

Figure 3 shows the actuator torque on the input shafts for CaPaMan prototype as function of time obtained obtained by simplified and complete dynamic models. These graphical presents a comparison between initial and optimal torque curves. It can be observed that the optimal values were strongly modified avoiding the abrupt variations of the initial curve. Moreover, it can be observed that dynamic models have great influence in the curves of the torques. Table 7 presents the average values of the torque for each leg mechanism, notice that the values obtained by using the complete model are higher than calculated with the simplified model.

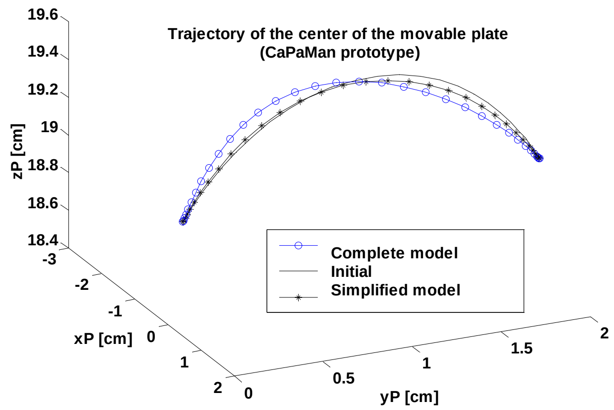

Figure 4- A 3D plot of the position of the center of the movable plate for CaPaMan prototype as function of time.

Application 2: Robust Hypothetical Manipulator

With the purpose of to emphasize the importance of a precise dynamic model, it was conceived a parallel architecture of CaPaMan that had great dimensions and consequently high values for the components mass. This structure named Robust Hypothetical Manipulator will be used in this application, your dimensional data are related in Table 4. It is adopted that the mobile platform has mass M=10.0 Kg, the segments h_i, b_i *and* c_i have masses respectively the same to m_{hi}=1.0 Kg, m_{bi}=0. 60 Kg and m_{ci}=1.0 Kg.

Table 4 – Dimensional parameters of the Robust Hypothetical Manipulator

$a_i = c_i$ [mm]	$b_i = d_i$ [mm]	h_i [mm]	$r_P = r_b$ [mm]	s_i [mm]
800	400	600	500	-100 ; 100

Table 5 – Optimal results for the Robust Hypothetical Manipulator (simplified dynamical model)

	Multi –objective function	Energy [Nm/s^2]	Total traveling time [s]	Jerk [rad/s^3]
Initial value	1.00	9212.7	0.30	1059.0
Optimal value	0.60	1934.7	0.44	252.4
Performance Index	40.0 %	79 %	-	76 %

Table 6 – Optimal results for the Robust Hypothetical Manipulator (complete dynamical model)

	Multi –objective function	Energy [Nm/s^2]	Total traveling time [s]	Jerk [rad/s^3]
Initial value	1.00	13386.0	0.30	910.5
Optimal value	0.64	3833.5	0.47	218.1
Performance Index	36 %	71 %	-	76 %

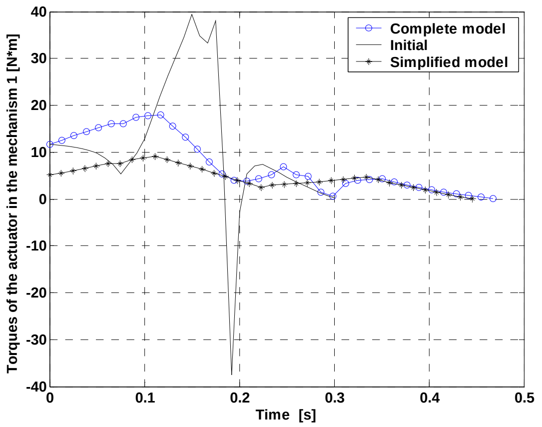

(a)

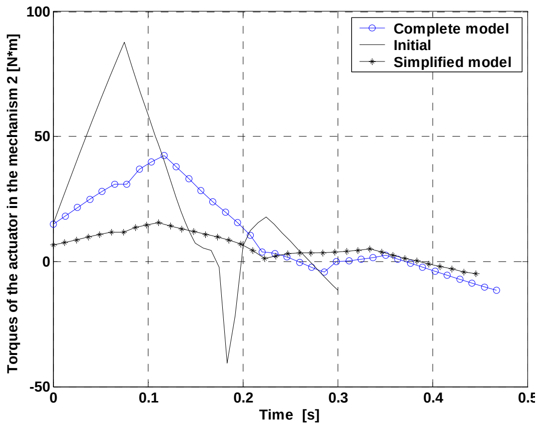

(b)

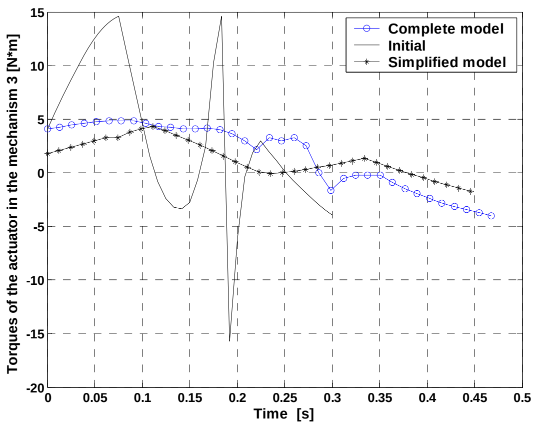

(c)

Figure 5-Optimum curves of the actuator torque for Robust Hypothetical Manipulator obtained by simplified and complete dynamic models: (a) leg mechanism 1; (b) leg mechanism 2; (c) leg mechanism 3.

The initial and optimal values for this application are shown in Table 5 for simplifies dynamical model and Table 6 for the complete model. Observe as the values of the energy and jerk are different for the two models, demonstrating the importance of taking in consideration the articulated parallelogram dynamic effects, mainly for robust structures. The results of the optimization process were very good, representing a great energy reduction.

In a similar way, the optimal curves obtained for the actuator torque on the input shafts are influenced by the adopted dynamic model, as can be seen in the Fig. 5. Also for this application, the optimization process produces smooth curves, avoiding the abrupt variations of the initial curve.

Finally, the Fig. 6 presents the initial and optimal position of the center of the movable plate for Robust Hypothetical Manipulator, considering the both models. Once again, it is demonstrated that the dynamic model should be calculated accurately because they modify the obtained results.

The average values of the torque for each leg mechanism are presented in Table 7, observe as the values are modified when the complete dynamical model is considered.

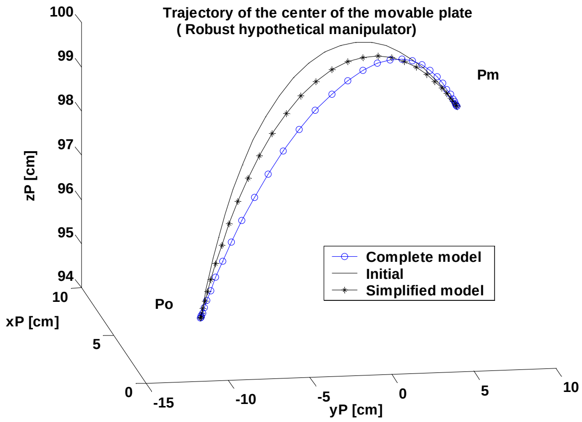

Figure 6- A 3D plot of the position of the center of the movable plate for Robust Hypothetical Manipulator.

Table 7 – Comparison of average torques for simplified and complete models

	Average torques (leg mechanism 1)	Average torques (leg mechanism 2)	Average torques (leg mechanism 3)
CaPaMan Prototype (Simplified Model)	0.1939	0.3953	0.1085
CaPaMan Prototype (Complete Model)	0.3548	0.6524	0.1806
Robust Manipulator (Simplified Model)	4.7567	6.7544	1.6853
Robust Manipulator (Complete Model)	7.9213	14.7554	3.2302

CONCLUSIONS

The results of the proposed optimum procedure show the soundness of the proposed formulation in order to further improve the dynamics performance of a parallel manipulator, to reduce energy consumption and to limit jerks during the motion. It is very important that the forces acting on the mobile platform are considered together with the forces on each articulated parallelogram of legs, because the results are strongly influenced by the adopted dynamic model.

ACKNOWLEDGMENTS

The second author is thankful to FAPEMIG for the partial financial support.

REFERENCES

Brobow, J.E.; Dubowsky, S.; Gibson, J.S., 1985. Time Optimal Control of Robotic Manipulators Along Specified Path.,k Int. Journal of Robotics Research, v.4, n.3, pp:3-17.

Byun, Y.K., Cho, H.S., 1997. “Analysis of a Novel 6-dof, 3-PPSP Parallel Mainpulator”, The International J. of Robotics Research, 16(6), pp.859-872.

Carvalho, J.C.M., Ceccarelli, M., 1999, “A Dynamic Analysis for Cassino Parallel Manipulator”, 10th IFToMM World Congress, Oulu, Vol.3, pp. 1202-1207.

Carvalho, J.C.M. and Ceccarelli, M., 2001, “A Closed Form Formulation for the Inverse Dynamics of Cassino Parallel Manipulator”, J. Multibody System Dynamics, Vol. 5, No. 2.

Ceccarelli, M., 1997, “A New 3 dof Spatial Parallel Mechanism”, Mechanism and Machine Theory, Vol. 32, No. 8, 895-902.

Clavel, R., 1987. "Un Nouveau Robot Très Rapide", Institut de Microtechnique, Ecole Polytechnique Fédérale de Lausanne, Suíça.

Clavel, R., 1988. "DELTA: A Fast Robot with Parallel Geometry", in Proceedings of 18th Int. Symp. on Industrial Robots, Lausanne, pp.91-100.

Constantinescu, D.; Croft, E.A., 2000. Smooth and Time-Optimal Trajectory Planning for Industrial Maniupaltors along Specified Paths. Journal of Robotic Systems. V.7, n.5, pp:233-249.

Di Gregorio, R.; Parenti-Castelli, 2004. "The 3-RRS wrist: a new, simple and non-overconstrained spherical parallel manipulator". Journal of Mechanical Design. Transactions of the ASME, v.126, n. 5, p. 850-855.

Eschenauer, H., Koski, J. and Osyczka, A., 1990, " Multicriteria Design Optimization", Berlin, Springer-Verlag.

Foley, J.D., Van Dam, A., Feiner, S. K. and Hughes, J. F., 1990, "Computer Graphics: Principles and Practice", 2nd Ed., Addison-Wesley Publishing Company, ISBN 0-201-12110-7.

Gosselin, C.M., Kong, X., Foucault, S., Bonev, I.A., 2004. "A Fuly-Decoupled 3-dof Translational Parallel Mechanism". In. Chemnitz Parallel Kinematics Seminar, 4., R. Neugebauer (ed.), Chemnitz, Germany, April 20-21, Proceedings. IWU vol. 24, p. 595-610.

Jacquet, P., Danescu, G., Carvalho, J.C.M., Dahan, M., 1992. "A Spatial Fully Parallel Manipulator", in Proceedings of World Congress on the Theory of Machines and Mechanisms, Udine.

Kim, H.S., Tsai, L.-W., 2002. "Design Optimization of a Cartesian Parallel Manipulator", In. 2002 ASME DETC, 29-1 Sep. 2002, Montreal, Canada. Proceedings.

Lallemand, J.P., Goudali, A., Zeghloul, S., 1997. "The 6-dof 2-DELTA Parallel Robot", Robotica 15, pp.407-416.

Merlet, J.P., Gosselin, C., 1991. "Nouvelle Architecture Pour Manipulateur Parallèle a Six Degrées de Liberté", Mechanism and Machine Theory 26(1), pp.77-90.

Pierrot, F., Dauchez, P., Fournier, A., 1991. "Hexa: A Fast Six-Dof Fully Parallel Robot", in Proceedings of Int. Conference on Advanced Robotics , Pisa, pp.1159-1163.

Portman, V., Sandler, B.Z., 1999. "High-Stiffness Precision Actuator for Small Displacements", Int. J. of Machine Tools & Manufacture, n.5, vol.39, pp.823-837.

Romiti, A., Sorli, M., 1992. "A Parallel 6-dof Manipulator for Cooperative Work Between Robots in Deburring", in Proceedings of 23rd Int. Symp. on Industrial Robots, Barcelona, pp.437-444.

Saramago S.F.P., Ceccarelli M., "An Optimum Robot Path Planning with Payload Constraints", International Journal Robotica, vol. 20, p. 395-404, 2002.

Shiller, Z.; Lu, H.H., 1992. Computation of Path Constrained Time-Optimal Motions with Dynamic Singularities. ASME Trans., Journal of Dynamic Systems, Meas., and Control. V.114, n.1, pp:34-40

Tsai, L.W., 1999, "Robot Analysis: The Mechanics of Serial and Parallel Manipulators", John Wiley & Sons, New York.

RESPONSIBILITY NOTICE

The authors are the only responsible for the printed material included in this paper.